NeuroImage: Clinical 18 (2018) 254–261

Contents lists available at ScienceDirect

NeuroImage: Clinical

journal homepage: www.elsevier.com/locate/ynicl

Altered brain high-energy phosphate metabolism in mild Alzheimer's disease: A 3-dimensional ^{31}P MR spectroscopic imaging study

Anne Rijpma[a,b,*], Marinette van der Graaf[c,d], Olga Meulenbroek[a,b], Marcel G.M. Olde Rikkert[a,b,1], Arend Heerschap[c,1]

[a] Department of Geriatric Medicine, Radboud university medical center, Nijmegen, The Netherlands
[b] Radboudumc Alzheimer Center, Donders Institute for Brain, Cognition and Behaviour, Radboud university medical center, Nijmegen, The Netherlands
[c] Department of Radiology and Nuclear Medicine, Radboud university medical center, Nijmegen, The Netherlands
[d] Department of Paediatrics, Radboud university medical center, Nijmegen, The Netherlands

ARTICLE INFO

Keywords:
Dementia
Alzheimer's disease
Phospholipid metabolism
Energy metabolism
Phosphorus magnetic resonance spectroscopic imaging

ABSTRACT

In Alzheimer's disease (AD), defects in essential metabolic processes for energy supply and phospholipid membrane function have been implicated in the pathological process. However, post-mortem investigations are generally limited to late stage disease and prone to tissue decay artifacts. In vivo assessments of high energy phosphates, tissue pH and phospholipid metabolites are possible by phosphorus MR spectroscopy (^{31}P–MRS), but so far only small studies, mostly focusing on single brain regions, have been performed. Therefore, we assessed phospholipid and energy metabolism in multiple brain regions of 31 early stage AD patients and 31 age- and gender-matched controls using ^{31}P–MRS imaging. An increase of phosphocreatine (PCr) was found in AD patients compared with controls in the retrosplenial cortex, and both hippocampi, but not in the anterior cingulate cortex. While PCr/inorganic phosphate and pH were also increased in AD, no changes were found for phospholipid metabolites. This study showed that PCr levels are specifically increased in regions that show early degeneration in AD. Together with an increased pH, this indicates an altered energy metabolism in mild AD.

1. Introduction

Alzheimer's disease (AD) is the main cause of dementia in the elderly, responsible for about half of the nearly 47 million dementia cases worldwide (Report, 2015). Although the disease is defined by the accumulation of amyloid beta plaques and neurofibrillary tau tangles in the brain (Braak and Braak, 1991), other pathological processes can be identified such as oxidative stress, vascular dysfunction, and inflammation (Akiyama et al., 2000; de la Torre, 2004; Markesbery, 1997). Additionally, defects in essential metabolic processes for energy supply and membrane function have been implicated in AD (Lynn et al., 2010; Nitsch et al., 1992).

The human brain is highly vulnerable to disturbances in energy metabolism, due to its relatively large energy consumption. Previous AD studies demonstrated alterations in global and cellular energy metabolism. FDG-PET studies have shown glucose hypometabolism in the retrosplenial cortex (RSC) and medial temporal lobe in people with mild cognitive impairment (MCI) and AD patients, as well as in cognitively normal carriers of the APOE ε4 allele (Nestor et al., 2003; Pietrini et al., 2000; Reiman et al., 2001; Reiman et al., 2005). Furthermore, the enzyme creatine kinase (CK), obtained from post-mortem AD tissue, shows reduced activity compared with samples that are free from neurological disease (Aksenov et al., 2000; David et al., 1998). The CK reaction, key to balance brain energy metabolism, can quickly replenish adenosine triphosphate (ATP) from the energy buffer phosphocreatine (PCr), when local energy demands suddenly increase (Lowe et al., 2015). This reaction also enhances the efficiency of mitochondrial oxidative phosphorylation (OXPHOS) by keeping adenosine diphosphate (ADP) sufficiently available (Schlattner et al., 2006) and prevents acidification by maintaining pH (for a review see

Abbreviations: ^{1}H, proton; ^{31}P–MRS, phosphorus magnetic resonance spectroscopy; AC, anterior commissure; ACC, anterior cingulate cortex; AD, Alzheimer's disease; ADP, adenosine diphosphate; ATP, adenosine triphosphate; CK, creatine kinase; Cr, creatine; CSF, cerebrospinal fluid; GM, grey matter; GPCh, glycerophosphocholine; GPEth, glycerophosphoethanolamine; HL, left hippocampus; HR, right hippocampus; LS, least square; MCI, mild cognitive impairment; MMSE, Mini Mental State Examination; MRSI, magnetic resonance spectroscopic imaging; NAD(H), nicotinamide adenine dinucleotide; OXPHOS, oxidative phosphorylation; PC, posterior commissure; PCh, phosphocholine; PCr, phosphocreatine; PDE, phosphodiesters; PEth, phosphoethanolamine; Pi, inorganic phosphate; PME, phosphomonoesters; ROI, region of interest; RSC, retrosplenial cortex; WM, white matter

* Corresponding author at: Radboud University Medical Center, Dep. Geriatric Medicine, - hp 925, P.O.Box 9101, 6500 HB Nijmegen, the Netherlands.
E-mail address: Anne.Rijpma@radboudumc.nl (A. Rijpma).

[1] Shared last author.

https://doi.org/10.1016/j.nicl.2018.01.031
Received 30 June 2017; Received in revised form 15 December 2017; Accepted 24 January 2018
Available online 28 February 2018

Wallimann et al., 2011).

One of the earliest pathological changes in AD is synaptic dysfunction, which correlates well with cognitive dysfunction and disease severity (Terry et al., 1991). Alterations in neuronal membrane composition, vital for synaptic transmission, have been linked to synaptic dysfunction in AD (Pomponi et al., 2008). For instance, post mortem studies found reduced levels of the major membrane components phosphatidylcholine, phosphatidylethanolamine and phosphatidylinositol (Nitsch et al., 1992; Pettegrew et al., 2001), as well as altered activity of catabolic and anabolic enzymes, suggesting compensatory metabolic changes to reduce the rate of neuronal membrane loss (Ross et al., 1998).

High energy phosphates, such as ATP and PCr, and metabolites of phospholipid membrane metabolism can be assessed in vivo by phosphorus magnetic resonance spectroscopy (^{31}P–MRS). This technique has been applied in AD (e.g. Forlenza et al., 2002; Mandal et al., 2012; Pettegrew et al., 1994; Smith et al., 1995), but previous studies, essentially focusing on single brain regions, were severely hampered by small sample sizes and low spectral resolution, resulting in a wide disparity in findings. Furthermore, differences in the control groups that were used, in the brain regions that were studied and in the disease stages and medication statuses of the patients, may have contributed to apparent inconsistencies in the literature.

The aim of the current study was to investigate whether abnormal phospholipid and energy metabolism can be detected non-invasively in early stage AD patients by ^{31}P MR spectroscopic imaging (^{31}P–MRSI). This investigation was designed to overcome the limitations of previous studies. First, we performed the measurements at 3 T field strength with proton (^{1}H) decoupling to increase spectral resolution and sensitivity. Secondly, by applying ^{31}P–MRS in a 3-dimensional imaging mode we could investigate multiple brain regions simultaneously. We specifically addressed regions that are of interest in AD, namely, the hippocampus, the RSC, and the anterior cingulate cortex (ACC). Finally, we selected a well-defined drug-naïve patient group and an age- and gender-matched control group.

2. Materials and methods

2.1. Subjects and design

All visits of patients and controls to the Radboud university medical center (Nijmegen, the Netherlands) took place between 2012 and 2015. Patients aged ≥50 years with a diagnosis of possible or probable AD according to the revised National Institute of Neurological and Communicative Disorders and Stroke and the Alzheimer's Disease and Related Disorders Association 2011 criteria (McKhann et al., 2011) with evidence of the pathophysiological process (i.e. from structural MRI or cerebrospinal fluid biomarker assays) and with a minimum Mini Mental State Examination (MMSE) score of 20, were recruited from the hospital's memory clinic or by referral from regional hospitals. All AD patients participated in a randomized controlled trial on the effect of a medical food on brain phospholipid metabolism (Rijpma et al., 2017; Dutch Trial Register 3346). Only baseline data were used in the current study. Healthy control subjects, age- and gender-matched to the AD group, were screened by telephone before being invited to the clinic. All subjects were drug-naïve for AD medication (cholinesterase inhibitors and NMDA-antagonists) and were free from neurological or psychiatric disorders (other than dementia, for the AD patients). Patients nor healthy controls used nutritional supplements containing docosahexaenoic acid, eicosapentaenoic acid or > 200% of the recommended daily allowance of vitamins B, C, or E. All subjects were screened for MRI contra-indications before inclusion in the study.

Written informed consent was obtained from all subjects and from the informal caregivers of the AD patients. The local ethics committee reviewed and approved the protocol and the study was conducted in accordance with the Declaration of Helsinki.

Medical history, medication use and MMSE were recorded from all subjects, as well as date of birth, sex, ethnicity, smoking habits, alcohol consumption, and family history of AD. Level of education was classified according to Verhage (Verhage, 1964) (comparable with the International Standard Classification of Education) and categorized in three groups: primary education or lower (low), junior vocational training (middle), and senior vocational or academic training (high).

2.2. MR acquisition

MRI and MRS were performed on a Magnetom Tim Trio 3T MR system (Siemens, Erlangen, Germany) with a dual-tuned ^{1}H/^{31}P volume head coil (Rapid Biomedical, Wuerzburg, Germany). High resolution MR images were acquired with a T1-weighted magnetisation-prepared rapid gradient-echo sequence (TR = 2300 ms, TE = 3.16 ms, TI = 1100 ms, 15° flip-angle, 176 sagittal slices, slice-matrix size = 256 × 256 mm, slice thickness = 1 mm, voxel-size = 1 × 1 × 1 mm, TA = 6:25 min).

^{31}P-MR spectra were acquired with whole brain 3D MRSI (a pulse-acquire sequence with 40° flip-angle, acquisition delay of 0.7 ms including 0.3-ms gradient phase encoding time, 512 ms acquisition duration with WALTZ4 ^{1}H decoupling during the first 256 ms with $\gamma B1 = 250$ Hz ensuring $(\gamma B1)^2 > (J_{PH})^2$, TR = 2000 ms, FOV 260 × 260 × 260 mm; matrix size = 10 × 10 × 10, acquisition time 13:08 min). Prior to acquisition, an automatic procedure was applied to optimize the magnetic field homogeneity of a rectangular shim volume maximizing brain coverage while bound by the skull. Subsequently, if necessary, the field homogeneity was further adjusted manually until a value of < 25 Hz was obtained for the full width at half maximum of the absolute-value ^{1}H MR water signal. K-space was sampled with a weighted elliptical phase-encoding scheme with four averages. The volume of interest was centered on the midline and parallel to the line from the anterior commissure to the posterior commissure. Spatial post-processing consisted of zerofilling to a matrix size of 16 × 16 × 16. The nominal volume of the measured voxels is about 17.5 cm^3, the effective voxel at 64% of the spatial response function has a spherical shape with a volume of about 40 cm^3 (Pohmann and von Kienlin, 2001).

2.3. MRS and MRI data analyses

Four regions of interest (ROI) were selected for analysis from the 3D ^{31}P–MRSI data: ACC, RSC, and left and right hippocampus (HL and HR). Guided by the T1-weighted images, the MRSI grid was shifted in the x, y and z dimension to position voxels in the ROI's (by AR; Fig. 1). For the ACC, a voxel was selected anterior to the genu of the corpus callosum, with the inferior border aligned with the line from the anterior commissure to the posterior commissure (AC-PC line), and on the midsagittal plane. For the RSC, a voxel on the midsagittal plane was selected posterior to the splenium of the corpus callosum, with the inferior border aligned with the AC-PC line. For the HL and HR, a voxel was selected at the anterior end of each hippocampus, with the inferior and lateral border of the voxel aligned with the inferior and lateral side of the hippocampus.

The software package Metabolite Report (Siemens Healthcare, Erlangen, Germany) was used for post-processing (i.e. 100 ms exponential filter, zero-filling, phase correction, baseline correction) and for automatic fitting of the spectra in the time-domain using prior knowledge appropriate for ^{31}P MR spectra (own spectral data and from de Graaf (2008)). Eleven well-resolved resonance peaks were fitted: the phospholipid metabolites phosphoethanolamine (PEth), phosphocholine (PCh), glycerophosphoethanolamine (GPEth) and glycerophosphocholine (GPCh), the high-energy phosphorus molecules PCr, ATP (α-ATP, β-ATP and γ-ATP), nicotinamide adenine dinucleotide (NAD(H)) and inorganic phosphate (Pi), and membrane-bound phospholipid (details of this procedure are described in the Appendix).

Both a quantitative evaluation of the fitting results and a visual quality control were performed. Quantitatively, only metabolite fits

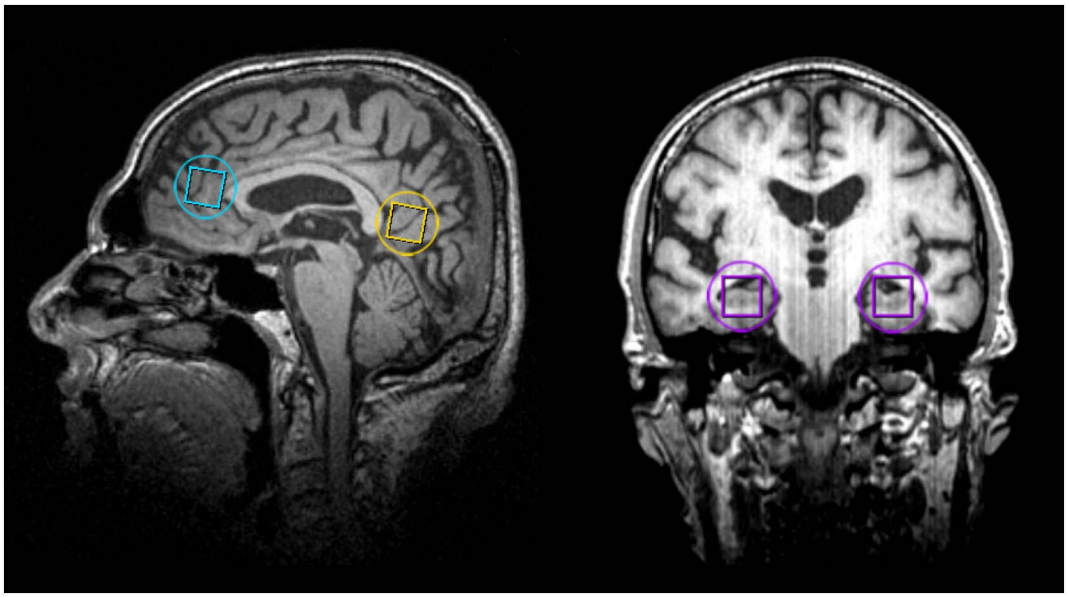

Fig. 1. Voxel selection of ^{31}P MR spectra displayed on sagittal (left) and coronal (right) anatomical images: anterior cingulate cortex (blue), retrosplenial cortex (yellow), left and right hippocampus (purple). The nominal voxel size is indicated by squares and an approximation of the effective spherical voxel size is indicated by circles. (For interpretation of the references to color in this figure legend, the reader is referred to the web version of this article.)

with a Cramer–Rao lower bound of ≤30% were considered reliable. Qualitatively, two MR spectroscopists (AR and MvdG) independently checked the spectra by visual inspection of the original spectra and the fitting results. If a metabolite peak was visually present, and its fit was assigned to the correct resonance—giving a minimal residue in the subtraction spectrum—the fitting result was accepted.

The integral of each metabolite resonance was expressed as a percent area of the total phosphorous signal in the corresponding spectrum. Hereby, the data were normalized, and corrected for cerebrospinal fluid (CSF) content and thus for differences in local atrophy. Phosphomonoesters (PME) were calculated from the sum of PEth and PCh, phosphodiesters (PDE) from GPEth and GPCh and total ATP (tATP) from the sum of α-ATP, β-ATP and γ-ATP. In addition, the ratios PME/PDE, PE/GPE, PC/GPC and PCr/Pi were computed. Intracellular pH was determined from the chemical shift difference between the PCr and Pi resonance peaks (Petroff et al., 1985).

The T_1-weighted images were segmented into grey matter (GM), white matter (WM) and CSF using automatic segmentation software (by AR; SPM8, Welcome Trust Centre for Neuroimaging, London, UK; VBM8, Structural Brain Mapping Group, Jena, USA). Binary tissue maps (matrices) of GM, WM, CSF were convolved with the, digitally sampled, mathematically-modelled three dimensional point-spread function of the MRSI, using Matlab 2012b (The Mathworks, Inc., Matrick, MA), to obtain theoretically correct values of the contribution of tissue type to each ROI (each consisting of one MRS voxel). GM-to-WM ratio (GM/WM) was calculated for each ROI for each subject.

2.4. Statistical analyses

Two-factorial mixed ANOVAs were used to test differences in tissue content (GM, WM, and CSF) and GM/WM in each ROI between mild AD patients and controls. Group and brain region (ROI) differences were analyzed for each spectroscopy outcome parameter using a mixed model with group (AD or control), sex, brain region and its interaction with group as fixed factors, considering brain region as a within subject factor, and adjusting for age. An unstructured variance-covariance matrix for brain region was selected. The group-by-brain region interaction was only kept in the model if $p < 0.10$. In the covariate analysis, GM/WM in each ROI was added to the final primary model of each parameter, to investigate the effect of tissue composition on the effects of group and brain region. Although the inclusion of GM/WM in the final model led to a small change (10–20%) in many parameter estimates, this was mainly without a change in main and/or interaction effects. Therefore we report the primary model in tables and figures and refer to the effect of GM/WM only where it led to a change in the main and/or interaction effects, and with > 20% change in the parameter estimates of group or brain region. Goodness of fit was assessed by comparing Bayesian Information Criteria (BIC) and homoscedasticity and normality of residuals were assessed by visual inspection. Statistical analyses were performed using SAS 9.2 Software for Windows (SAS Institute Inc., Cary, NC, USAf). Statistical significance was set at $p < 0.05$ without correction for multiple testing.

3. Results

3.1. Subjects

A total of 33 mild AD patients and 35 healthy control subjects were enrolled in the study and subjected to MRI and MRS measurements. Two AD patients had MR spectra of low quality (due to severe motion and a dental implant) and four control subjects were found to meet an exclusion criterion during or after the visit (two subjects took nutritional supplements, two subjects presented with structural neurological damage from ischemic infarcts and trauma). Therefore, 31 AD patients and 31 controls were included in the final analysis. The groups were similar with respect to age and gender (see Table 1 for subject characteristics).

3.2. ROI tissue contribution

The interaction between group and brain region for GM and CSF contributions to the total volume of each ROI was not significant, but GM and CSF differed significantly between groups, and between brain regions (all $p < 0.001$). GM was lower and CSF was higher in AD patients than in healthy control subjects (mean % ± SD, GM:36.3 ± 4.7 vs. 40.5 ± 4.0; CSF: 22.5 ± 4.7 vs. 18.1 ± 3.5). overall, GM was highest in the right hippocampus, followed by left hippocampus, and then followed by equal amounts in RSC and ACC (data not shown). CSF in RSC and ACC was higher than in both hippocampi. There was a significant interaction between group and brain region for WM

Table 1
Subject characteristics.

	AD $n = 31$	Controls n = 31
Age	73.4 years (6.8)	73.5 years (6.3)
Gender (%)	13 males (42%)	15 males (48%)
MMSE	23.2 (2.0)	28.1 (1.4)
Time since AD diagnosis	1.6 months [0.2–15.3]	–
BMI	25.4 kg/m^2 (3.8)	26.3 kg/m^2 (4.5)
Educational level (low/middle/high)	9/16/6	4/9/18
Smoking (never/past/current)	13/17/1	6/22/3
≥1 relatives with AD (n)	19	7

MMSE, mini mental state examination; AD, Alzheimer's disease; BMI, body mass index. Data are presented as mean (standard deviation) or median [range] unless otherwise indicated.

($p = 0.004$) and GM/WM ($p = 0.021$). WM was higher in AD patients compared with controls in the right hippocampus (41.5 ± 3.0 vs. 40.0 ± 2.6), but not in the other brain regions. GM/WM was lower in AD patients than in controls in ACC, and both hippocampi, but not in RSC (data not shown).

3.3. MRS results

High quality MR spectra were obtained with well-resolved PME, PDE, Pi, PCr and ATP signals for the brain regions evaluated in this study (Fig. 2). The linewidth of PCr varied between 8 and 13 Hz in the different brain regions (ACC: mean ± SD 13.5 ± 3.3 Hz, RSC: 8.1 ± 2.6 Hz, HL: 11.2 ± 2.6 Hz, HR: 12.5 ± 3.0 Hz). We did not observe a difference in the linewidth of PCr between AD and controls (mean ± SD 11.5 ± 3.9 Hz and 11.1 ± 3.0 Hz, not tested). ROI tissue contributions showed typical differences with lower GM and higher CSF in AD patients compared with controls.

In the statistical analysis, the interaction between group and brain region was kept in the model for PCr, γATP and βATP, because it survived our criterion of $p < 0.10$. For all other outcome parameters, the interaction term had a p-value > 0.10 and was removed from the model.

3.4. Differences in energy metabolites and pH between groups

A significant interaction between group and brain region was found for PCr, showing that normalized PCr signals were higher in mild AD patients compared with healthy control subjects in the RSC (Least Square (LS) mean difference = 0.86, SEM = 0.29, $p = 0.004$), HL (LS mean difference = 1.52, SEM = 0.52, $p = 0.005$) and HR (LS mean difference = 1.47, SEM = 0.38, $p < 0.001$), but not in the ACC ($p = 0.947$) (Fig. 3A). The interaction between group and brain region was not significant for γATP and βATP. A main effect of group was found for PCr/Pi, showing that this ratio was higher in mild AD patients compared with healthy controls (LS mean difference = 0.22, SEM = 0.11, $p = 0.046$) (Fig. 3B). Also pH was increased in AD patients compared with controls (LS mean difference = 0.008, SEM = 0.004, $p = 0.032$) (Fig. 3C). No group differences were found for γATP, βATP, αATP, total ATP, Pi, and NAD(H) (all $p > 0.05$). For a summary of group effects see Table 2.

3.5. Differences in phospholipid metabolites between groups

No interaction or group difference between mild AD patients and healthy control subjects were found for any of the phospholipid metabolites (PEth, PCh, GPEtn, GPCh, PME, and PDE; Table 2) or their ratios (PEth/GPEth, PCh/GPCh, and PME/PDE) (all $p > 0.05$).

3.6. Differences in phosphorus metabolites and pH between brain regions

Brain region significantly affected all outcome parameters (all $p < 0.05$), except PCh and PME ($p > 0.05$). The normalized signals of total ATP, αATP, βATP, γATP, NAD(H), PEth, GPEtn, GPCh, and PDE were lower in the RSC than in the ACC and both hippocampi (all $p < 0.05$), while the pattern was reversed for the ratios PCh/GPCh and PME/PDE ($p < 0.001$). We found no difference between the left and right hippocampus for any of the energy and phospholipid metabolites or pH ($p > 0.05$), except for αATP (LS mean difference = 0.65, SEM = 0.26, $p = 0.015$). See Table 3 for an overview of the differences between brain regions.

3.7. Influence of tissue content

In the covariate analysis GM/WM was added to the final model. This did not change the effects of group, brain region or the interaction between group and brain region on PCr, Pi, total ATP, αATP, βATP, γATP, NAD(H), pH or any of the phospholipid metabolite signals. However, for PCr/Pi the main effect of brain region was reduced to a trend ($p = 0.062$) and the parameter estimates changed substantially, when GM/WM was included in the model. There was no change in the effect of group on PCr/Pi.

4. Discussion

In this study we acquired high-quality ^{31}P-MRSI data of the brain in a large group of mild AD patients and in a well-matched healthy elderly population. High spectral resolution enabled us to gather information on high-energy phosphates, as well as on specific phospholipid metabolites. MR spectra of the four brain regions that are among the most studied in AD were investigated and for the first time, these areas were measured simultaneously by ^{31}P-MRSI. We detected increased phosphocreatine and pH, but no changes in phospholipid metabolite signals in mild AD patients. Interestingly, the increase in PCr was observed in the RSC and in the hippocampi, regions that both show early pathological changes in AD, but not in the ACC, a region known to be involved in the disease at a later stage. This suggests that the PCr abnormality expands across brain regions in a similar fashion as other AD pathologies, such as tau (Braak and Braak, 1991). Furthermore, in both groups pH, high energy phosphates, and most phospholipid metabolites differed across brain regions.

As in vivo human ^{31}P MRS brain studies are nearly always performed under signal saturating conditions, changes in T1 relaxation time may affect metabolite signal intensities (Longo et al., 1993). Although we cannot exclude that such an effect has contributed to the increased PCr signal, it would require a rather drastic decrease in PCr's T1 value from about 3 to 2 s. Moreover, no increases in PME and PDE signals were detected, while those would be affected more severely by a T1 decrease (Klomp et al., 2008). A potential cause for relaxation enhancement is a higher brain iron accumulation in AD patients (Tao et al., 2014), but this would increase the signal linewidth, which was not observed. Thus, the most likely explanation for the increased PCr signal is a higher tissue concentration of this compound.

Elevated PCr signals have been reported before for AD patients in comparison with young controls (Mandal et al., 2012), but as PCr also increases with age in healthy persons (Chiu et al., 2015; Forester et al., 2010; Longo et al., 1993) it is unclear whether this finding was due to an aging effect. The current results showed increased PCr, and PCr/Pi, in AD patients compared with elderly controls of the same age. In contrast, two earlier studies showed a decrease in prefrontal PCr in mild, but not severe, AD (Pettegrew et al., 1994) and decreased PCr/Pi in the frontal lobe (Smith et al., 1995). However, these studies were performed at 1.5 T with only surface coil localization and involved small sample sizes.

As the concentration of high energy phosphates depends on the

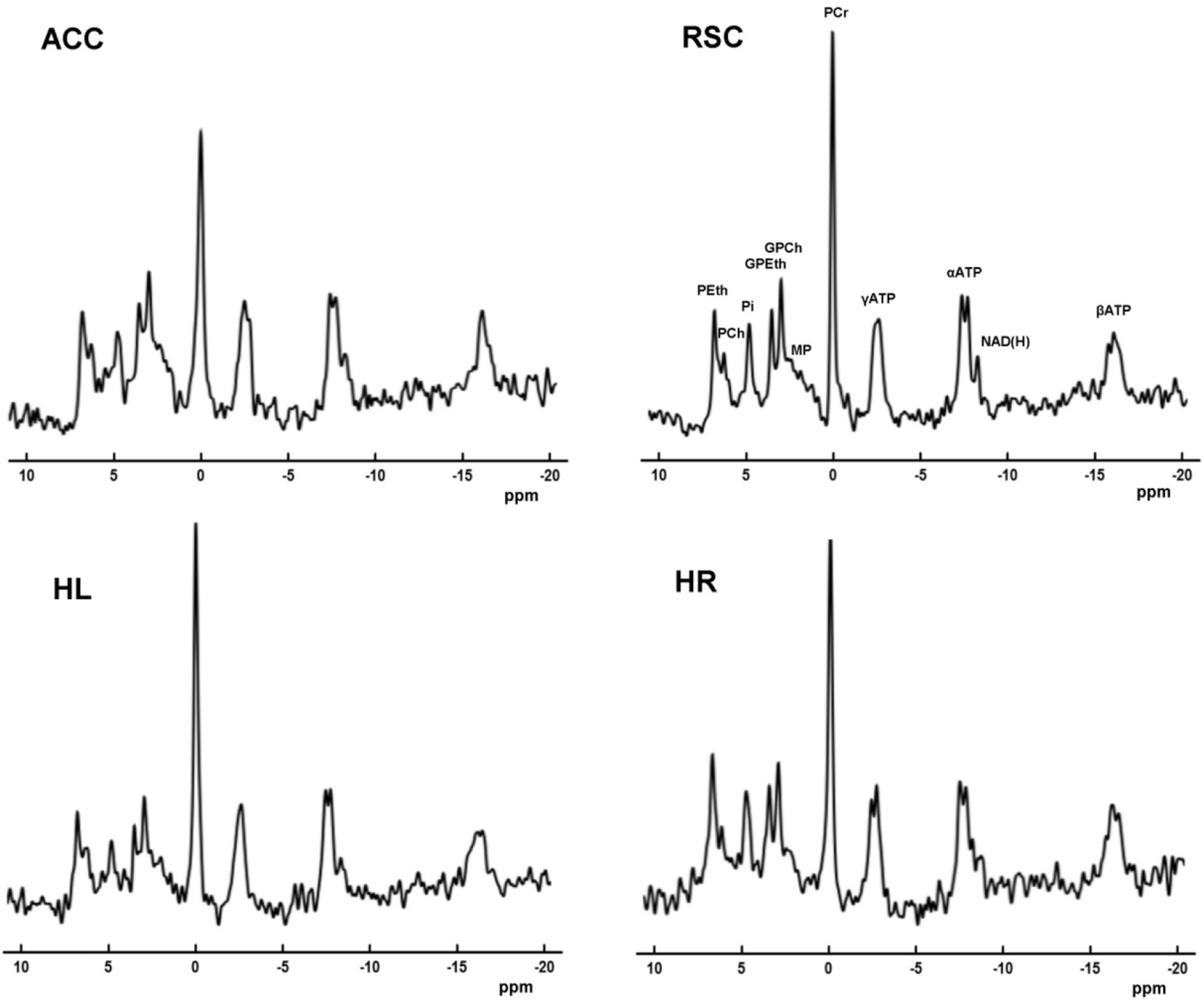

Fig. 2. Representative spectra from the anterior cingulate cortex (ACC), retrosplenial cortex (RSC), left hippocampus (HL) and right hippocampus (HR) of an Alzheimer's disease patient (73 years old). Zero filling to 4096 data points and an 8 Hz Gaussian filter were applied for display purposes. PEth, phosphoethanolamine; PCh, phosphocholine; Pi, inorganic phosphate; GPEth, glycerophosphoethanolamine; GPCh, glycerophosphocholine; MP, membrane phospholipids; PCr, Phosphocreatine; ATP, adenosine triphosphate; NAD(H), nicotinamide adenine dinucleotide; ppm, parts per million.

balance between energy production and energy utilization, increases in steady state PCr levels and PCr/Pi reflect a redistribution in the content of metabolites involved in the connected CK and ATPase pseudo-equilibria (Du et al., 2007). This may be the consequence of reduced utilization of ATP (Forester et al., 2010), caused by synaptic dysfunction or loss of other energy requiring functionalities (Chandrasekaran et al., 1996; Rapoport et al., 1996). Although these changes are expected to lower ATP production and thus PCr, the final balance between reduced energy production and consumption may still result in a higher PCr level. To maintain equilibrium, the increased PCr should be accompanied by changes in the levels of other substrates of the CK reaction, such as a higher ATP concentration. Previous studies reported an increase in (γ)ATP (Mandal et al., 2012; Mecheri et al., 1997; Pettegrew et al., 1994), although no alterations in ATP levels were found in the current nor in several other studies (e.g. Forlenza et al., 2002; Gonzalez et al., 1996; Smith et al., 1995). Alternatively, a higher PCr may result from an increased total amount of cellular creatine (Cr). However, in vivo measurements of total Cr content in MCI and AD patients provide no clear evidence that Cr is increased in the disease (Graff-Radford and Kantarci, 2013; Tumati et al., 2013). Finally, decreases in ADP and/or H^+ concentration may accompany the PCr increase. Indeed, a slight increase in pH was detected in mild AD patients, but it does not fully compensate for the increase in PCr when equilibrium is assumed. Changes in PCr levels have also been associated with decreased CK activity in the AD brain (Forester et al., 2010; Mandal et al., 2012). However, it is unlikely to be a direct effect of this decrease as even in cytosolic CK knockout mice the remaining CK activity (< 20%) is sufficient to preserve equilibrium (in 't Zandt et al., 2004). Clearly, a strongly affected reaction rate will affect processes that require rapid (local) energy supply, and a higher PCr level may represent a flux adaptation to this condition.

There is some evidence for involvement of PCr in processes beyond the PCr-CK system. Since glutamate uptake by synaptic vesicles is stimulated by PCr, independent of ATP or CK (Xu et al., 1996), increased PCr may prevent glutamate excitotoxicity (Bender et al., 2005). Furthermore, PCr may be able to bind to and stabilize phospholipid membranes (Tokarska-Schlattner et al., 2005) and may function as an osmolyte (Bothwell et al., 2001) and a neurotransmitter (Almeida et al., 2006). In addition, differences in metabolite levels may be explained by variations in tissue and cell type (Griffin et al., 2002; Urenjak et al., 1993), although our results remained unchanged when adjusting for grey and white matter. A prominent neuropathological feature in AD is astrogliosis (Osborn et al., 2016). As this alters the neuron-to-glia ratio within grey and white matter (Beach et al., 1989), it is possible that morphological differences between AD patients and healthy aged controls play a role in the alterations in PCr and pH. Furthermore, atrophy may introduce slight differences in the brain area that the measured volumes encompass, which effect may not be entirely captured by

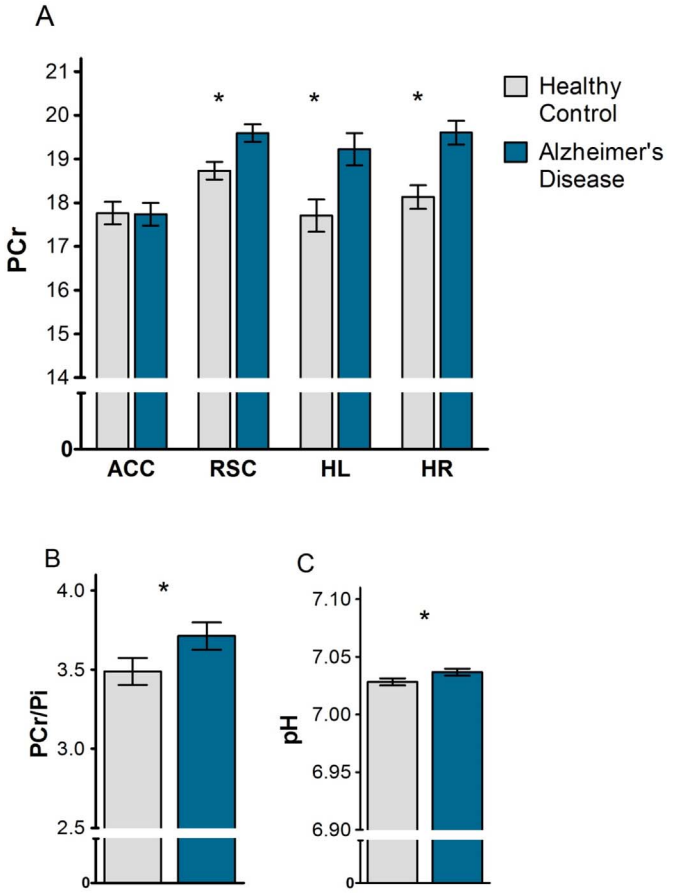

Fig. 3. Normalized phosphocreatine (PCr; A), ratio of PCr to inorganic phosphate (PCr/Pi; B) and pH (C) in patients with Alzheimer's disease (AD) and healthy control (HC) subjects. PCr was normalized by expressing the integral as a percent area of the total phosphorous signal in the corresponding spectrum. Data represent Least Square means ± SEM, *$p < 0.05$ AD vs HC. ACC, anterior cingulate cortex; RSC, retrosplenial cortex; HL, left hippocampus; HR, right hippocampus.

adjusting for grey and white matter. However, ROIs were placed such that volume of the actual area of interest was maximized and the measured signals are dominated by the reported brain regions of interest.

Contrary to our expectation, we did not observe differences between mild AD patients and controls in any of the phospholipid metabolites, although preclinical and post-mortem studies show alterations in membrane function and lipid composition in AD (Nitsch et al., 1992; Ross et al., 1998). No previous in vivo studies have reported on PEth, PCh, GPEth or GPCh, but several studies reported changes of their total amounts, i.e. PME, PDE or their ratio, in AD (e.g. Forlenza et al., 2005; Gonzalez et al., 1996; Mecheri et al., 1997), although others reported no differences in these metabolites (Bottomley et al., 1992; Brown et al., 1993; Murphy et al., 1993; Smith et al., 1995). The most consistent finding seems to be an increase in total PME in the prefrontal cortex in AD compared with elderly controls (Cuenod et al., 1995; Forlenza et al., 2005; Pettegrew et al., 1994). In the present study, part of the frontal cortex was covered in the ACC measurement, but we did not find changes in PEth, PCh, nor total PME. However, changes in the complex phospholipid cycle may be too small at this disease stage to be detected with the current methodology. Although we had sufficient spectral resolution to resolve the phosphomonoester signal of PEth and PCh, and the phosphodiesters signal of GPEth and GPCh, these may still reflect metabolites connected to different phospholipid pools. Moreover, differential expression of phosphatidylethanolamine and phosphatidylcholine species across hippocampal subfields was recently shown in AD (Mendis et al., 2016).

Table 2
Main effect of group (healthy controls vs Alzheimer's disease) on phosphorus metabolite signals and tissue pH for all investigated regions.

	AD	Control	p-Value
PCr*	19.04 ± 0.18 *n = 124*	18.08 ± 0.18 *n = 124*	**< 0.001**
Pi	5.30 ± 0.11 *n = 121*	5.47 ± 0.11 *n = 123*	0.240
PCr/Pi	3.71 ± 0.09 *n = 121*	3.49 ± 0.09 *n = 123*	**0.046**
total ATP	42.88 ± 0.27 *n = 124*	43.17 ± 0.27 *n = 124*	0.445
NAD(H)	3.96 ± 0.11 *n = 103*	4.09 ± 0.11 *n = 96*	0.388
PEth	8.19 ± 0.11 *n = 119*	8.33 ± 0.11 *n = 122*	0.375
PCh	3.90 ± 0.07 *n = 112*	3.93 ± 0.07 *n = 114*	0.757
GPEth	4.32 ± 0.11 *n = 109*	4.31 ± 0.11 *n = 117*	0.942
GPCh	5.96 ± 0.15 *n = 108*	6.08 ± 0.15 *n = 109*	0.526
pH	7.037 ± 0.003 *n = 121*	7.028 ± 0.003 *n = 123*	**0.032**

LS means ± SEM of metabolite levels, as percentage of total phosphorus signal in the corresponding spectrum, in patients with Alzheimer's disease and healthy control subjects. Significant group effects ($p < 0.05$, AD versus Control) indicated in bold. *PCr also has a significant interaction between group and brain region. LS, least squares; SEM, standard error of the mean; n, number of observations; AD, Alzheimer's disease; HC, healthy control; PCr, Phosphocreatine; Pi, inorganic phosphate; ATP, adenosine triphosphate; NAD(H), nicotinamide adenine dinucleotide; PEth, phosphoethanolamine; PCh, phosphocholine; GPEth, glycerophosphoethanolamine; GPCh, glycerophosphocholine.

MRSI revealed that high energy phosphates, pH and most phospholipid metabolites vary extensively across brain regions that are of interest in AD. These differences existed in both mild AD patients and controls, and were not explained by regional variation in grey and white matter content, with the ratio PCr/Pi as the sole exception. This indicates that the investigated regions are metabolically different from each other. It also underlines that regional differences should be taken into account in any cross-sectional or longitudinal metabolic study. Moreover, as shown here for PCr, changes in metabolite levels in disease may not be the same for all brain regions.

The current study only reports on relative metabolite levels, as obtaining absolute quantifications requires several assumptions, which adds complexity and reduces reliability. Moreover, when the variation in atrophy between and within groups is large, relative measurements are preferred over absolute. A second limitation may be that our results have not been corrected for multiple testing, because of the exploratory nature of this study. Replication of these results in an independent population would strengthen our findings. In future research it would be valuable to include preclinical AD patients or an at-risk population to clarify the disease stage in which abnormalities in PCr and pH appear, as well as perform longitudinal (intervention) studies to follow these abnormalities. In addition, magnetization transfer experiments to determine the CK and ATPase reaction rates with measurements of absolute concentrations of PCr and ATP to determine fluxes (Du et al., 2007), would elucidate whether the dynamics of the PCr-CK and ATPases systems are affected in AD.

4.1. Conclusion

To the best of our knowledge, this is the largest study to date investigating brain phospholipid and energy metabolism in AD by ^{31}P MRS. Increased PCr levels were found in regions that show early degeneration in AD, but not in the ACC, a region known to be involved in this disease at a later stage. Together with an increased pH, this indicates that energy metabolism is altered in mild AD. Although most

Table 3
Main effect of brain region on phosphorus signal integrals and tissue pH.

	ACC	RSC	HL	HR	p-Value
PCr*	17.75 ± 0.18†,‡,§	19.16 ± 0.14¶	18.47 ± 0.26	18.87 ± 0.19	< **0.001**
	n = 62	*n = 62*	*n = 62*	*n = 62*	
Pi	5.34 ± 0.12	5.65 ± 0.10¶	5.21 ± 0.16	5.34 ± 0.18	**0.027**
	n = 61	*n = 62*	*n = 61*	*n = 60*	
PCr/Pi	3.42 ± 0.09‡,§	3.46 ± 0.07$^{\P,\#}$	3.76 ± 0.14	3.76 ± 0.12	**0.009**
	n = 61	*n = 62*	*n = 61*	*n = 60*	
total ATP	42.58 ± 0.38†,‡,§	40.06 ± 0.33$^{\P,\#}$	45.24 ± 0.38	44.21 ± 0.41	< **0.001**
	n = 62	*n = 62*	*n = 62*	*n = 62*	
NAD(H)	4.39 ± 0.12†	3.47 ± 0.11$^{\P,\#}$	4.17 ± 0.16	4.08 ± 0.14	< **0.001**
	n = 49	*n = 61*	*n = 45*	*n = 44*	
PEth	8.45 ± 0.18†	7.81 ± 0.12$^{\P,\#}$	8.31 ± 0.15	8.46 ± 0.18	< **0.001**
	n = 61	*n = 62*	*n = 60*	*n = 58*	
PCh	3.99 ± 0.10	3.96 ± 0.10	3.94 ± 0.09	3.76 ± 0.11	0.429
	n = 55	*n = 61*	*n = 56*	*n = 54*	
GPEth	4.76 ± 0.15†,§	3.72 ± 0.09$^{\P,\#}$	4.42 ± 0.13	4.36 ± 0.11	< **0.001**
	n = 51	*n = 61*	*n = 57*	*n = 57*	
GPCh	6.69 ± 0.26†	5.01 ± 0.12$^{\P,\#}$	6.11 ± 0.15	6.28 ± 0.16	< **0.001**
	n = 46	*n = 61*	*n = 56*	*n = 54*	
pH	7.023 ± 0.004‡,§	7.017 ± 0.002$^{\P,\#}$	7.039 ± 0.004	7.050 ± 0.005	< **0.001**
	n = 61	*n = 62*	*n = 61*	*n = 60*	

LS means ± SEM of metabolite levels, as percentage of total phosphorus signal in the corresponding spectrum, in anterior cingulate cortex, retrosplenial cortex and hippocampi. Significant ($p < 0.05$) main effect of brain region indicated in bold. *PCr also has a significant interaction between group and brain region. $p < 0.05$, ACC vs †RSC, ‡HL, or §HR; RSC vs ¶HL, or $^{\#}$HR. LS, least squares; SEM, standard error of the mean; n, number of observations; ACC, anterior cingulate cortex; RSC, retrosplenial cortex; HL, left hippocampus; HR, right hippocampus; PCr, Phosphocreatine; Pi, inorganic phosphate; ATP, adenosine triphosphate; NAD(H), nicotinamide adenine dinucleotide; PEth, phosphoethanolamine; PCh, phosphocholine; GPEth, glycerophosphoethanolamine; GPCh, glycerophosphocholine.

phospholipid metabolites, like the high energy phosphates, differed between the investigated brain regions in both groups, no alterations in phospholipid metabolism were found specific to mild AD.

Acknowledgements

We thank all participants and their caregivers for participating in this study. The authors are indebted to Jack van Asten, Miriam Lagemaat and Bart Philips (department of Radiology and Nuclear Medicine, Radboud university medical center) for their help in developing the acquisition and post-processing protocols and Rianne de Heus (department of Geriatric Medicine, Radboud university medical center) for her assistance during data acquisition and analysis. We thank the Institute of Nuclear Sciences Applied to Health and the Visual Neurosciences Lab, Institute for Biomedical Imaging and Life Sciences (University of Coimbra, Coimbra, Portugal) for providing us with spectroscopic co-registry software.

Funding

This work was supported by Nutricia Research. They had no role in the analysis and interpretation of the data, or in writing this report.

Declaration of interest

Conflicts of interest: none

Appendix A. Supplementary data

Supplementary data to this article can be found online at https://doi.org/10.1016/j.nicl.2018.01.031.

References

Akiyama, H., Barger, S., Barnum, S., Bradt, B., Bauer, J., Cole, G.M., Cooper, N.R., Eikelenboom, P., Emmerling, M., Fiebich, B.L., Finch, C.E., Frautschy, S., Griffin, W.S.T., Hampel, H., Hull, M., Landreth, G., Lue, L.F., Mrak, R., Mackenzie, I.R., McGeer, P.L., O'Banion, M.K., Pachter, J., Pasinetti, G., Plata-Salaman, C., Rogers, J., Rydel, R., Shen, Y., Streit, W., Strohmeyer, R., Tooyoma, I., Van Muiswinkel, F.L., Veerhuis, R., Walker, D., Webster, S., Wegrzyniak, B., Wenk, G., Wyss-Coray, T., Neuroinflammation Working, G., 2000. Inflammation and Alzheimer's disease. Neurobiol. Aging 21 (3), 383–421. http://dx.doi.org/10.1016/s0197-4580(00)00124-x.

Aksenov, M., Aksenova, M., Butterfield, D.A., Markesbery, W.R., 2000. Oxidative modification of creatine kinase BB in Alzheimer's disease brain. J. Neurochem. 74 (6), 2520–2527.

Almeida, L.S., Salomons, G.S., Hogenboom, R., Jakobs, C., Schoffelmeer, A.N.M., 2006. Exocytotic release of creatine in rat brain. Synapse 60 (2), 118–123. http://dx.doi.org/10.1002/syn.20280.

Beach, T.G., Walker, R., McGeer, E.G., 1989. Patterns of gliosis in Alzheimer's disease and aging cerebrum. Glia 2 (6), 420–436. http://dx.doi.org/10.1002/glia.440020605.

Bender, A., Auer, D.P., Merl, T., Reilmann, R., Saemann, P., Yassouridis, A., Bender, J., Weindl, A., Dose, M., Gasser, T., Klopstock, T., 2005. Creatine supplementation lowers brain glutamate levels in Huntington's disease. J. Neurol. 252 (1), 36–41. http://dx.doi.org/10.1007/s00415-005-0595-4.

Bothwell, J.H., Rae, C., Dixon, R.M., Styles, P., Bhakoo, K.K., 2001. Hypo-osmotic swelling-activated release of organic osmolytes in brain slices: implications for brain oedema in vivo. J. Neurochem. 77 (6), 1632–1640. http://dx.doi.org/10.1046/j.1471-4159.2001.00403.x.

Bottomley, P.A., Cousins, J.P., Pendrey, D.L., Wagle, W.A., Hardy, C.J., Eames, F.A., McCaffrey, R.J., Thompson, D.A., 1992. Alzheimer dementia - quantification of energy-metabolism and mobile phosphoesters with P-31 NMR-spectroscopy. Radiology 183 (3), 695–699.

Braak, H., Braak, E., 1991. Neuropathological staging of Alzheimer-related changes. Acta Neuropathol. 82 (4), 239–259.

Brown, G.G., Garcia, J.H., Gdowski, J.W., Levine, S.R., Helpern, J.A., 1993. Altered brain energy metabolism in demented patients with multiple subcortical ischemic lesions - working hypotheses. Arch. Neurol. 50 (4), 384–388.

Chandrasekaran, K., Hatanpää, K., Brady, D.R., Rapoport, S.I., 1996. Evidence for physiological down-regulation of brain oxidative phosphorylation in Alzheimer's disease. Exp. Neurol. 142 (1), 80–88. http://dx.doi.org/10.1006/exnr.1996.0180.

Chiu, P.W., Chi, A., Law, K., Shiu, J., Kwan, K., Chuen, R., Chang, C., Chu, L.W., Fung Mak, H.K., 2015. 31P magnetic resonance spectroscopy on normal aging human brain at 3.0T. Alzheimers Dement. 11 (7, Supplement), 549–550. http://dx.doi.org/10.1016/j.jalz.2015.06.699.

Cuenod, C.A., Kaplan, D.B., Michot, J.L., Jehenson, P., Leroywillig, A., Forette, F., Syrota, A., Boller, F., 1995. Phospholipid abnormalities in early Alzheimers-disease - in vivo phosphorus-31 magnetic-resonance spectroscopy. Arch. Neurol. 52 (1), 89–94.

David, S., Shoemaker, M., Haley, B.E., 1998. Abnormal properties of creatine kinase in Alzheimer's disease brain: correlation of reduced enzyme activity and active site photolabeling with aberrant cytosol-membrane partitioning. Brain research. Mol. Brain Res. 54 (2), 276–287.

Du, F., Zhu, X.-H., Qiao, H., Zhang, X., Chen, W., 2007. Efficient in vivo 31P magnetization transfer approach for noninvasively determining multiple kinetic parameters and metabolic fluxes of ATP metabolism in the human brain. Magn. Reson. Med. 57 (1), 103–114. http://dx.doi.org/10.1002/mrm.21107.

Forester, B.P., Berlow, Y.A., Harper, D.G., Jensen, J.E., Lange, N., Froimowitz, M.P., Ravichandran, C., Iosifescu, D.V., Lukas, S.E., Renshaw, P.F., Cohen, B.M., 2010. Age-related changes in brain energetics and phospholipid metabolism. NMR Biomed. 23 (3), 242–250 (doi:10.1002/nbm.1444).

Forlenza, O.V., Wacker, P., Nunes, P.V., Gattaz, W.F., Bottino, C.M.C., Castro, C.C., Cerri,

G.G., 2002. Abnormal phospholipid metabolism in Alzheimer's disease: 31P-spectroscopy study of the pre-frontal cortex. Neurobiol. Aging 23 (1) (S463-S).
Forlenza, O.V., Wacker, P., Nunes, P.V., Yacubian, J., Castro, C.C., Otaduy, M.C.G., Gattaz, W.F., 2005. Reduced phospholipid breakdown in Alzheimer's brains: a P-31 spectroscopy study. Psychopharmacology 180 (2), 359–365. http://dx.doi.org/10.1007/s00213-005-2168-8.
Gonzalez, R.G., Guimaraes, A.R., Moore, G.J., Crawley, A., Cupples, L.A., Growdon, J.H., 1996. Quantitative in vivo P-31 magnetic resonance spectroscopy of Alzheimer disease. Alzheimer Dis. Assoc. Disord. 10 (1), 46–52. http://dx.doi.org/10.1097/00002093-199603000-00008.
de Graaf, R., 2008. In Vivo NMR Spectroscopy. Principles and Techniques, Second Edition. John Wiley, Chichester.
Graff-Radford, J., Kantarci, K., 2013. Magnetic resonance spectroscopy in Alzheimer's disease. Neuropsychiatr. Dis. Treat. 9, 687–696 (doi:10.2147/NDT.S35440).
Griffin, J.L., Bollard, M., Nicholson, J.K., Bhakoo, K., 2002. Spectral profiles of cultured neuronal and glial cells derived from HRMAS H-1 NMR spectroscopy. NMR Biomed. 15 (6), 375–384. http://dx.doi.org/10.1002/nbm.792.
Klomp, D.W., Wijnen, J.P., Scheenen, T.W., Heerschap, A., 2008. Efficient 1H to 31P polarization transfer on a clinical 3T MR system. Magn. Reson. Med. 60 (6), 1298–1305. http://dx.doi.org/10.1002/mrm.21733.
Longo, R., Ricci, C., Dalla Palma, L., Vidimari, R., Giorgini, A., den Hollander, J.A., Segebarth, C.M., 1993. Quantitative 31P MRS of the normal adult human brain. Assessment of interindividual differences and ageing effects. NMR Biomed. 6 (1), 53–57.
Lowe, M.T.J., Faull, R.L.M., Christie, D.L., Waldvogel, H.J., 2015. Distribution of the Creatine transporter throughout the human brain reveals a Spectrum of Creatine transporter immunoreactivity. J. Comp. Neurol. 523 (5), 699–725. http://dx.doi.org/10.1002/cne.23667.
Lynn, B.C., Wang, J., Markesbery, W.R., Lovell, M.A., 2010. Quantitative changes in the mitochondrial proteome from subjects with mild cognitive impairment, early stage, and late stage Alzheimer's disease. Journal of Alzheimers Disease 19 (1), 325–339. http://dx.doi.org/10.3233/jad-2010-1254.
Mandal, P.K., Akolkar, H., Tripathi, M., 2012. Mapping of hippocampal pH and neurochemicals from in vivo multi-voxel P-31 study in healthy normal young male/female, mild cognitive impairment, and Alzheimer's disease. Journal of Alzheimers Disease 31, S75–S86. http://dx.doi.org/10.3233/jad-2012-120166.
Markesbery, W.R., 1997. Oxidative stress hypothesis in Alzheimer's disease. Free Radic. Biol. Med. 23 (1), 134–147. http://dx.doi.org/10.1016/s0891-5849(96)00629-6.
McKhann, G.M., Knopman, D.S., Chertkow, H., Hyman, B.T., Jack, C.R., Jr., Kawas, C.H., Klunk, W.E., Koroshetz, W.J., Manly, J.J., Mayeux, R., Mohs, R.C., Morris, J.C., Rossor, M.N., Scheltens, P., Carrillo, M.C., Thies, B., Weintraub, S., Phelps, C.H. 2011. The diagnosis of dementia due to Alzheimer's disease: recommendations from the National Institute on Aging-Alzheimer's Association workgroups on diagnostic guidelines for Alzheimer's disease. Alzheimers Dement. 7(3), 263–9. doi:https://doi.org/10.1016/j.jalz.2011.03.005.
Mecheri, G., MarieCardine, M., SappeyMarinier, D., Bonmartin, H., Albrand, G., Ferry, G., CoppardMeyer, N., Courpron, P., 1997. In vivo hippocampal P-31 NMR metabolites in Alzheimer's disease and ageing. European Psychiatry 12 (3), 140–148. http://dx.doi.org/10.1016/s0924-9338(97)80203-9.
Mendis, L.H.S., Grey, A.C., Faull, R.L.M., Curtis, M.A., 2016. Hippocampal lipid differences in Alzheimer's disease: a human brain study using matrix-assisted laser desorption/ionization-imaging mass spectrometry. Brain Behav 6, 1–17. http://dx.doi.org/10.1002/brb3.517. e00517.
Murphy, D.G., Bottomley, P.A., Salerno, J.A., DeCarli, C., Mentis, M.J., Grady, C.L., Teichberg, D., Giacometti, K.R., Rosenberg, J.M., Hardy, C.J., et al., 1993. An in vivo study of phosphorus and glucose metabolism in Alzheimer's disease using magnetic resonance spectroscopy and PET. Arch. Gen. Psychiatry 50 (5), 341–349.
Nestor, P.J., Fryer, T.D., Ikeda, M., Hodges, J.R., 2003. Retrosplenial cortex (BA 29/30) hypometabolism in mild cognitive impairment (prodromal Alzheimer's disease). Eur. J. Neurosci. 18 (9), 2663–2667. http://dx.doi.org/10.1046/j.1460-9568.2003.02999.x.
Nitsch, R.M., Blusztajn, J.K., Pittas, A.G., Slack, B.E., Growdon, J.H., Wurtman, R.J., 1992. Evidence for a membrane defect in Alzheimer-disease brain. Proc. Natl. Acad. Sci. U. S. A. 89 (5), 1671–1675. http://dx.doi.org/10.1073/pnas.89.5.1671.
Osborn, L.M., Kamphuis, W., Wadman, W.J., Hol, E.M., 2016. Astrogliosis: an integral player in the pathogenesis of Alzheimer's disease. Prog. Neurobiol. 144, 121–141. http://dx.doi.org/10.1016/j.pneurobio.2016.01.001.
Petroff, O.A.C., Prichard, J.W., Behar, K.L., Alger, J.R., den Hollander, J.A., Shulman, R.G., 1985. Cerebral intracellular pH by 31P nuclear magnetic resonance spectroscopy. Neurology 35 (6), 781. http://dx.doi.org/10.1212/wnl.35.6.781.
Pettegrew, J.W., Panchalingam, K., Klunk, W.E., McClure, R.J., Muenz, L.R., 1994. Alterations of cerebral metabolism in probable Alzheimer's disease: a preliminary study. Neurobiol. Aging 15 (1), 117–132. http://dx.doi.org/10.1016/0197-4580(94)90152-x.
Pettegrew, J.W., Panchalingam, K., Hamilton, R.L., McClure, R.J., 2001. Brain membrane phospholipid alterations in Alzheimer's disease. Neurochem. Res. 26 (7), 771–782 (doi:10.1023/a:1011603916962).
Pietrini, P., Alexander, G.E., Furey, M.L., Hampel, H., Guazzelli, M., 2000. The neurometabolic landscape of cognitive decline: in vivo studies with positron emission tomography in Alzheimer's disease. Int. J. Psychophysiol. 37 (1), 87–98. http://dx.doi.org/10.1016/S0167-8760(00)00097-0.
Pohmann, R., von Kienlin, M., 2001. Accurate phosphorus metabolite images of the human heart by 3D acquisition-weighted CSI. Magn. Reson. Med. 45 (5), 817–826. http://dx.doi.org/10.1002/mrm.1110.
Pomponi, M., Bria, P., Pomponi, M., 2008. Is Alzheimer's disease a synaptic disorder? Journal of Alzheimers Disease 13 (1), 39–47.
Rapoport, S.I., Hatanpaa, K., Brady, D.R., Chandrasekaran, K., 1996. Brain energy metabolism, cognitive function and down-regulated oxidative phosphorylation in Alzheimer disease. Neurodegeneration 5 (4), 473–476. http://dx.doi.org/10.1006/neur.1996.0065.
Reiman, E.M., Caselli, R.J., Chen, K., Alexander, G.E., Bandy, D., Frost, J., 2001. Declining brain activity in cognitively normal apolipoprotein E epsilon 4 heterozygotes: a foundation for using positron emission tomography to efficiently test treatments to prevent Alzheimer's disease. Proc. Natl. Acad. Sci. U. S. A. 98 (6), 3334–3339. http://dx.doi.org/10.1073/pnas.061509598.
Reiman, E.M., Chen, K., Alexander, G.E., Caselli, R.J., Bandy, D., Osborne, D., Saunders, A.M., Hardy, J., 2005. Correlations between apolipoprotein E epsilon4 gene dose and brain-imaging measurements of regional hypometabolism. Proc. Natl. Acad. Sci. U. S. A. 102 (23), 8299–8302. http://dx.doi.org/10.1073/pnas.0500579102.
Report, World Alzheimer, 2015. The Global Impact of Dementia: An Analysis of Prevalence, Incidence, Cost and Trends. Alzheimer's Disease International (ADI), London.
Rijpma, A., van der Graaf, M., Lansbergen, M.M., Meulenbroek, O., Cetinyurek-Yavuz, A., Sijben, J.W., Heerschap, A., Olde Rikkert, M.G.M., 2017. The medical food Souvenaid affects brain phospholipid metabolism in mild Alzheimer's disease: results from a randomized controlled trial. Alzheimer's Research & Therapy 9, 51. http://dx.doi.org/10.1186/s13195-017-0286-2.
Ross, B.M., Moszczynska, A., Erlich, J., Kish, S.J., 1998. Phospholipid-metabolizing enzymes in Alzheimer's disease: increased lysophospholipid acyltransferase activity and decreased phospholipase A(2) activity. J. Neurochem. 70 (2), 786–793.
Schlattner, U., Tokarska-Schlattner, M., Wallimann, T., 2006. Mitochondrial creatine kinase in human health and disease. Biochim Biophys Acta-Mol Basis Dis 1762 (2), 164–180. http://dx.doi.org/10.1016/j.bbadis.2005.09.004.
Smith, C.D., Pettigrew, L.C., Avison, M.J., Kirsch, J.E., Tinkhtman, A.J., Schmitt, F.A., Wermeling, D.P., Wekstein, D.R., Markesberry, W.R., 1995. Frontal-lobe phosphorus-metabolism and neuropsychological function in aging and in Alzheimers-disease. Ann. Neurol. 38 (2), 194–201. http://dx.doi.org/10.1002/ana.410380211.
Tao, Y., Wang, Y., Rogers, J.T., Wang, F., 2014. Perturbed iron distribution in Alzheimer's disease serum, cerebrospinal fluid, and selected brain regions: a systematic review and meta-analysis. J. Alzheimers Dis. 42 (2), 679–690 (doi:10.3233/jad-140396).
Terry, R.D., Masliah, E., Salmon, D.P., Butters, N., Deteresa, R., Hill, R., Hansen, L.A., Katzman, R., 1991. Physical basis of cognitive alterations in Alzheimers-disease - synapse loss is the major correlate of cognitive impairment. Ann. Neurol. 30 (4), 572–580. http://dx.doi.org/10.1002/ana.410300410.
Tokarska-Schlattner, M., Wallimann, T., Schlattner, U., 2005. Membrane protective effects of phosphocreatine. In: Biophysical Society Annual Meeting. Biophysal Journal.
de la Torre, J.C., 2004. Is Alzheimer's disease a neurodegenerative or a vascular disorder? Data, dogma, and dialectics. Lancet Neurol. 3 (3), 184–190.
Tumati, S., Martens, S., Aleman, A., 2013. Magnetic resonance spectroscopy in mild cognitive impairment: systematic review and meta-analysis. Neurosci. Biobehav. Rev. 37 (10 Pt 2), 2571–2586 (doi:10.1016/j.neubiorev.2013.08.004).
Urenjak, J., Williams, S.R., Gadian, D.G., Noble, M., 1993. Proton nuclear-magnetic-resonance spectroscopy unambiguously identifies different neural cell-types. J. Neurosci. 13 (3), 981–989.
Verhage, F., 1964. Intelligentie en leeftijd: onderzoek bij Nederlanders van twaalf tot zevenenzeventig jaar. (Van Gorcum).
Wallimann, T., Tokarska-Schlattner, M., Schlattner, U., 2011. The creatine kinase system and pleiotropic effects of creatine. Amino Acids 40 (5), 1271–1296. http://dx.doi.org/10.1007/s00726-011-0877-3.
Xu, C.J., Klunk, W.E., Kanfer, J.N., Xiong, Q., Miller, G., Pettegrew, J.W., 1996. Phosphocreatine-dependent glutamate uptake by synaptic vesicles - a comparison with ATP-dependent glutamate uptake. J. Biol. Chem. 271 (23), 13435–13440.
in 't Zandt, H.J.A., Renema, W.K.J., Streijger, F., Jost, C., Klomp, D.W.J., Oerlemans, F., Van der Zee, C., Wieringa, B., Heerschap, A., 2004. Cerebral creatine kinase deficiency influences metabolite levels and morphology in the mouse brain: a quantitative in vivo H-1 and P-31 magnetic resonance study. J. Neurochem. 90 (6), 1321–1330. http://dx.doi.org/10.1111/j.1471-4159.2004.02599.x.